Ceramics International 44 (2018) 390–393

Contents lists available at ScienceDirect

Ceramics International

journal homepage: www.elsevier.com/locate/ceramint

The effect of Al_2O_3-MgO additives on the microstructure of spark plasma sintered silicon nitride

O.A. Lukianova*, O.N. Ivanov

Belgorod State National Research University, 85, Pobedy Str., 308015 Belgorod, Russia

ARTICLE INFO

Keywords:
Silicon nitride
Magnesium oxide
Microstructure
Spark plasma sintering

ABSTRACT

It was shown that spark plasma sintered silicon nitride with a high content of Al_2O_3 and MgO consists of α and β silicon nitride, the main phase being α silicon nitride. The increase in the sintering temperature did not lead to significant changes in the phase composition as occurs in silicon nitride added with Al_2O_3-Y_2O_3. It was found that increasing in SPS temperature above 1650 °C leads to an insignificant increase in the density. A complex shaped equiaxed grain microstructure was shown in both cases. However, doping with aluminum and yttrium oxides allows obtaining an elongated grain microstructure. The Hall-Petch effect was observed for the microhardness of the investigated SPSed silicon nitride. The microhardness of the described ceramics was rather high and more than 1900 HV compared to the pressureless sintered at 1800 °C silicon nitride with the microhardness equal to 1511 HV.

1. Introduction

Nowadays, silicon nitride has been studied extensively and widely used for high temperature applications due to its superior thermo-mechanical and tribological properties, namely, high-temperature strength, good oxidation resistance and low thermal expansion coefficient [1]. The control of mechanical properties as well as the microstructure of silicon nitride has been investigated extensively over the past few decades. It can be realized by using of various additives and different manufacturing methods. Mechanical properties of silicon nitride are determined by their microstructure meaning both grains and grain-boundary glass phase.

Magnesium oxide and aluminum oxide are the most promising sintering additives because of its relatively low cost. The influence of magnesium oxide on the microstructure and mechanical properties of silicon nitride a few have been reported [2,3], but, have not been as comprehensively studied as such compositions as MgO-Y_2O_3, Al_2O_3-Y_2O_3 [4–7]. Previous studies concerned with mostly on performing the fruitful complex of high strength and thermal stability of silicon nitride [8–15]. However, a few studies have been explored the correlation between the microstructure, phase composition and density with a temperature of spark plasma sintering of the aluminum oxide and magnesium oxide doped silicon nitride [16,17]. Relatively low sintering temperatures proposed in our study can be also justified by the fact that magnesium oxide reduces the melting point of the silicate glass on the surface of silicon nitride powder according to some Refs. [4,18].

It has been recognized that the reaction bounded silicon nitride (RBSN) has a constant strength in a wide range of temperatures despite on its relatively low mechanical properties compared with the hot isostatic pressed (HIPed) silicon nitride. However, HIPed silicon nitride had ultimate strength but the mechanical properties dramatically decrease with a slight increasing in temperature due to degradation of the glass phase. Thus, the absence of a glass phase is preferred and necessary in terms of potential high temperature applications.

The Spark Plasma Sintering (SPS) is one of the most promising alternatives to HIP and GP (gas pressure sintering) for sintering silicon nitride due to its low sintering time. Also the spark plasma sintering is characterized by such advantages as a relatively high sintering speed and comparatively low sintering temperature. Also it is possible to slow down the intensive grain growth of ceramics by SPS in contrast to traditional sintering methods. Nishimura et al. described dense silicon nitride manufactured by spark plasma sintering at 1550 °C during 5.5 min under 49 MPa minimized the grain growth during sintering and allowed the fabrication of dense silicon nitride [19].

Spark plasma sintered silicon nitride were selected as representative of ceramics have a large number of various commercial applications and frequently used in basic research of structure–property relationships. The choice for study only these two selected sintering temperatures was based on the interest in the effect of the investigated additives on the completeness of the α→β phase transformation of the silicon nitride.

The evaluation of the microstructure of spark plasma sintered

* Corresponding author.
E-mail address: sokos100@mail.ru (O.A. Lukianova).

http://dx.doi.org/10.1016/j.ceramint.2017.09.188
Received 31 August 2017; Received in revised form 20 September 2017; Accepted 22 September 2017
Available online 23 September 2017
0272-8842/ © 2017 Elsevier Ltd and Techna Group S.r.l. All rights reserved.

silicon nitride with an increased content of such cheap additives as alumina and magnesium oxide remains unclear and has attracted much interest. The aim of the current study is to clarify the effect of the self-made magnesium oxide and high content of aluminum oxide on the microstructure of the silicon nitride ceramics. Finally, the features of the microstructure and properties i.e. microhardness, density, morphology and average grain size of both produced ceramics, are presented and discussed.

It is important to note that described ceramics would be attractive for various high-temperature applications due to its fine equiaxed microstructure [7,20]. Another point in this study was a better understanding of the role of sintering additives in the densification and microstructural development of silicon nitride ceramics and the consequences for final properties [19].

2. Material and methods

Fine α -silicon nitride powder (92 wt%) was mixed with 2 wt% self-made MgO and 6 wt% Al_2O_3(A16 SG, 600 nm) using vibratory disc mill Retsch RS-200. Other details were reported previously [21–28]. A new innovative technology has been used to produce a nanoscale high-purity powder of magnesium oxide. In particular, proposed magnesium oxide powder was synthesized from the magnesium nitrate hexahydrate $Mg(NO_3)_2{\cdot}6H_2O$ leached in the nitric acid from the natural raw material of serpentinite after several cycles of magnetic separation. [25].

The sintering temperature was controlled by a pyrometer. Disc samples of 40 mm diameter were SPSed (Sumitomo Coal Mining Co. Ltd.) at 1550 °C and 1650 °C under 50 MPa during 10 min.

The samples were cut with a band saw from a sintered billet. The structural observations have been carried out with secondary electrons (SE) on the polished surfaces using a Quanta 600 FEG scanning electron microscope.

The density of the specimens was determined by helium pycnometry (Micromeritics Accu Pyc 1340). Crystalline phases were determined by X-ray diffraction (XRD, Rigaku Ultima IV).

Microhardness tests were carried out on samples using an automatic microhardness analysis system DM-8 at 30-N loads, a total of ten indentation points were made on the polished surface for each sample.

3. Results

Fig. 1 shows the microstructures of produced ceramics sintered at different temperatures. Their microhardness, densities, and average grain size are summarized in Table 1. The silicon nitride ceramics produced by SPS at 1550 °C is marked in Table 1 as SPS155, ceramics SPSed at 1650 °C is denoted as SPS165 and ceramics pressureless sintered at 1880 °C is referred as SN18 [26], respectively. Both ceramics demonstrate almost the same type of microstructure. SEM micrographs revealed the fine microstructure of the SPS155 with different amount of the complex form relatively large equiaxed grains with an average size of 440–600 nm and with a very small amount of elongated 1 μm grains. The microstructure of the SPS165 ceramics also consists of the nearly hexagonal large grains with the size ranged from 540 nm to 860 nm in addition to small amount of elongated grains with an average size of 1 μm. The lack of the surface porosity was observed for both investigated ceramics. The equiaxed α-Si_3N_4 grains connected randomly with each other and formed fine-grained microstructure that could be benefit for the various high-temperature applications of silicon nitride ceramics [26,28].

Table 1
Properties of produced silicon nitride ceramics.

Type	Method	Grain shape/average size	HV	g/cm^3	β- phase content, %	Ref.
SPS155	SPS	equiaxed 440–600 nm + elongated 1.0 μm	1957	3.13	11	This work
SPS165	SPS	equiaxed 540–860 nm + elongated 1.0 μm	1985	3.14	15	This work
SN18	Sintering	equiaxed 1.3 μm + elongated 2.6 μm	1511	3.03	100	[26]

The density of the obtained materials was nearly the same and equal to 3.13 g/cm^3 and 3.14 g/cm^3 for SPS155 and SPS165, respectively.

Only α and β silicon nitride were observed, however the major phase was α-Si_3N_4.

4. Discussion

Clarke and Thomas showed the features of the structure of MgO doped hot pressed silicon nitride and indicate that the second phase does not exist as a continuous wetting layer at the grain boundaries at room temperature, but is generally localized at some of the β-grain junctions and, occasionally, as a very thin layer between 2 grains [29].

The features of the structure of pressureless sintered silicon nitride with the same amount and type of additives have been discussed in more detail in our previous study. The microstructure of this silicon nitride is duplex and quite different compared to the described material and mostly consists of the equiaxed α-grains, while the secondary elongated β-grains can also be distinguished. The advantages and disadvantages of this material have been described elsewhere [26]. Different type of microstructure indicates a difference in the mechanisms of microstructure evolution for both corresponding sintering methods. The microstructure of the silicon nitride with various amounts of magnesium oxide has been also described in detail in our previous works [25]. We showed that the optimum content of magnesium oxide in the initial charge is equal to 2 wt% in terms of the linear shrinkage,

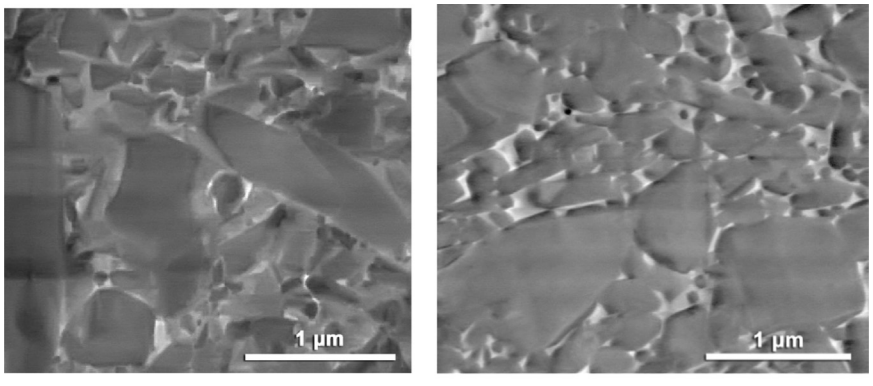

Fig. 1. Microstructure of the produced ceramics SPSed at a) 1550 °C b) 1650 °C.

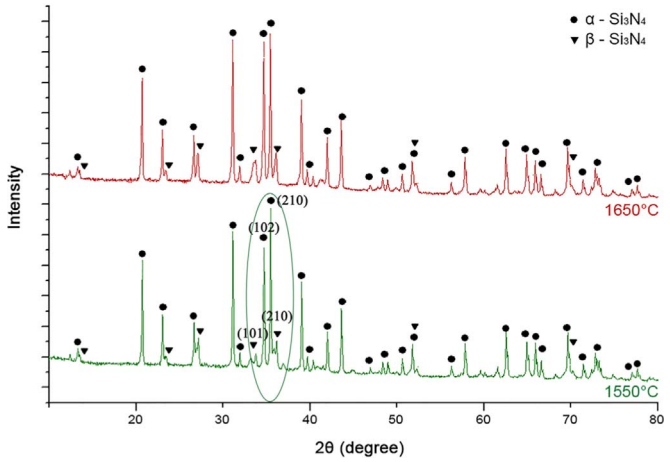

Fig. 2. XRD of the produced Si_3N_4 ceramics.

density and microstructural features.

The microstructure of the Al_2O_3-MgO doped silicon nitride ceramics SPSed at different sintering temperatures is shown in Fig. 1. The grain growth takes place when investigated ceramics are sintered above 1550 °C. Two types of grains were identified by SEM. The figure shows the nearly equiaxed α-Si_3N_4 structure (Fig. 1a and b). Grain-boundary glassy phase is also observed (white range around silicon nitride grains). It is also known that the composition of the grain-boundary and its thickness are characterized by the metal oxide additives, and in turn, the film thickness strongly depends on the chemical composition [29].

In contrast, the microstructure of the described earlier silicon nitride added with Al_2O_3-Y_2O_3 is characterized by the much larger content of the glass phase [27]. This factor is extremely important in terms of high-temperature and dielectric applications of silicon nitride ceramics because a major problem preventing its application is the dramatic decrease in strength of the hot-pressed form above 1000 °C. This decrease is generally attributed to the presence of a glassy phase between the silicon nitride grains.

Fig. 2 shows that there was no other phase in XRD patterns except of α-Si_3N_4 and β-Si_3N_4 despite on the content of sintering aids. The XRD analyses revealed α-Si_3N_4 as a major phase. The observed features of the phase composition can be explained in the first approximation according to the Kingery model explains the effect of magnesium oxide on the microstructure and phase composition of the silicon nitride. In particular, the addition of magnesium oxide in the silicon nitride is characterized by a solution-controlled mechanism and promotes the partial phase transformation and complete densification. In contrast, yttrium oxide leads to a full phase transformation of the silicon nitride and complete densification in accordance with the Kingery model. The sintering is controlled by a diffusion mechanism using Y_2O_3 [30]. It was reported that the α-silicon nitride ceramics are preferred as compared with the β silicon nitride due to its lower dielectric losses [20]. The slight grain growth was observed after spark plasma sintering.

Thus, aluminum oxide and magnesium oxide eventually leads to the optimal complex of the fine equiaxial structure and predominance of α-Si_3N_4 as the main phase beneficial for the dielectric properties of produced ceramics. In addition, the intensities of diffraction peaks of the β-Si_3N_4 increased with the increase of sintering temperature. The β-Si_3N_4 content was calculated by the following equation [31]:

$$R_\beta = \left[\frac{I_\beta(101) + I_\beta(210)}{I_\alpha(102) + I_\alpha(210) + I_\beta(101) + I_\beta(210)} \right] \quad (1)$$

The phase β-content R_β for SPS155 was 11%, while with increasing sintering temperature the β-phase content changed insignificantly according to Eq. (1) and became equal to 15% for SPS165. Yu et al. also described Si_3N_4 with the same oxides with the coexisted α-Si_3N_4 and β-Si_3N_4 in the samples. However, the content of the β-phase described in Ref. [4] was almost twice higher as our results. Li et al. [3] studied the microstructure of silicon nitride with Al_2O_3-MgO and MgO-$AlPO_4$ obtained by SPS at 1300 °C and 1400 °C. The features of the microstructure of silicon nitride presented by Li et al. in Ref. [3] are in good agreement with those described in our article. However, materials studied in Ref. [3] were characterized by a much higher porosity ranged from 2.1% to 29.6% as compared with our materials as it has been previously reported by the present authors [3]. The crystal phase $MgSiO_3$ was described in addition to α silicon nitride and β silicon nitride phases in Ref. [16] as a result of the reaction between magnesium oxide with silicon oxide on the surface of silicon nitride particles. The forming of the $MgSiO_3$ crystal phase as well as β-Si_3N_4 and $Si_2Al_4O_4N_4$ in silicon nitride SPSed at 1550 °C with a twice higher amount of MgO 4 wt% compared to our material and various contents of aluminum oxide was also proposed by Yan et al. The main phase of both silicon nitride described by these authors was α-Si_3N_4. They showed that a high content of alumina 6 wt% led to formation of a small amount of $Si_2Al_4O_4N_4$, while a small addition of aluminum oxide 2 wt% led to the absence of this SiAlON in the phase composition of reported silicon nitride [17]. Thus, lack of the $MgSiO_3$ in our material can be explained by the low content of magnesium oxide. The presence of a small amount of $Si_2Al_4O_4N_4$ in Ref. [17] can be presumably explained by a lower sintering temperature compared to our work. Peng et al. [32] reported about the microstructure of silicon nitride with $MgSiN_2$ SPSed in the temperature range from 1400 °C to 1600 °C. Silicon nitride ceramics sintered at 1400 °C during 6 min and sintered at 1500 °C during 3 min demonstrated both α-Si_3N_4 and β-Si_3N_4 while ceramics sintered at 1500 °C during 12 min were characterized only by single β-Si_3N_4 phase. This kinetics is generally explained in terms of the high sintering time. Silicon nitride sintered at a lower temperature 1400 °C has an equiaxial microstructure in accordance with the results described in our study. But ceramics sintered at a higher sintering temperature 1500 °C and 1600 °C had a bimodal structure with with a large number of elongated β-grains in contrast to described ceramics sintered at 1650 °C with predominantly equiaxial microstructure [32]. It should also be noted that an increase in the sintering temperature up to 1600 °C during 12 min led to significant grain growth as Peng et al. reported [32]. Thus, the nanosized self-made magnesium oxide powder and an increased amount of aluminum oxide powder used in our study presumably retards the phase transformation of the silicon nitride.

The density of the investigated ceramics also slightly increases from 3.13 g/cm^3 to 3.14 g/cm^3 (90.2% and 90.5% from the theoretical density, respectively) with an increase in the temperature of spark plasma sintering from 1550 °C to 1650 °C, which leads to more complete densification. The density of SPSed silicon with analogous additions described by Yu et al. [4], varied from ~ 80% to 97% depending on the sintering temperature ranged from 1400 °C to 1500 °C, respectively. The density of the SPSed silicon with 4 wt% MgO and 6 wt% of Al_2O_3 described by Yan et al. varied from ~ 76% to 96% depending on the sintering temperature ranged from 1300 °C to 1500 °C, respectively [17]. Normally, the kinetics of the sintering of silicon nitride is generally described by the liquid-phase mechanism. Miranzo et al. compared silicon nitride ceramics produced by HP and SPS, respectively. The complete grain boundary phase wetting of the SPSed silicon nitride was observed compared with the large glassy pockets of the silicon nitride in this article as well as in our present study [33]. This work also showed that improved densification taking place in the particle rearrangement stage of the liquid phase during SPS can be effectively explained by the increase of the liquid phase wetting and the capillary forces by the electric field [33].

Joshi et al. have carried out at a systematic study of the polycrystalline silicon nitride microstructure with Y_2O_3, Er_2O_3 and Nd_2O_3 and 3 wt% MgO and 9 wt% AlN produced by hot press sintering at 1850 °C under 30 MPa. It was found that grains of the reported ceramics are like interwoven and the grain growth is anisotropic [34].

The Hall-Petch relation for microhardness can be written as [35]:

$$H = H_0 + K_H \cdot d^{-1/2} \quad (2)$$

where H_0, and K_H are constants. Chu et al. showed that the Hall-Petch relationship was recognized for HPed, HPed/GPed and HPed/HIPed Si_3N_4 ceramics [36]. However, Bellosi et al. describe the inverse Hall's Petch relation for silicon nitride [37]. The microhardness of the produced ceramics insignificantly increases from 1957 HV to 1985 HV with an increase in the sintering temperature from 1550 °C to 1650 °C despite on the increase in density and the grain growth. Although, both SPSed samples are characterized by higher microhardness as compared with the pressureless sintered silicon nitride with a microhardness equal to 1511 HV with the same type and amount of additives described in our previous work [26].

5. Conclusions

In summary it is clearly seen that silicon nitride ceramics Al_2O_3-MgO doped with a fine microstructure and equiaxial grains with a complex shape have been fabricated by spark plasma sintering. An increase in the temperature of spark plasma sintering from 1550 °C to 1650 °C led to insignificant increase in the average grain size. The main results can be summarized as follows:

1. The main crystal phase of both produced ceramics was α-Si_3N_4. The microstructure of the produced ceramics with a predominance of the equiaxial α-silicon nitride grains observed. The features of the investigated microstructure in the first approximation can be interpreted within the framework of the Kingery model.
2. The microhardness of produced silicon nitride was high and more than 1900 HV and could be expressed by a Hall-Petch relationship in the context of comparison with the pressureless sintered at 1800 °C ceramics with a lower microhardness equal to 1511 HV.
3. It was shown that the self-made magnesium oxide and high content of aluminum oxide does not significantly affect the phase transformation of silicon nitride with an increase in the temperature of spark plasma sintering from 1550 °C to 1650 °C.

Acknowledgements

This work was supported by the Ministry of Education and Science of the Russian Federation (grant number No 3.6586.2017/BY).

References

[1] H. Kita, K. Hirao, H. Hyuga, M. Hotta, N. Kondo, Review and Overview of Silicon Nitride and SiAlON, Including Their Applications. Handbook of Advanced Ceramics, Elsevier, 2013, pp. 245–266, http://dx.doi.org/10.1016/B978-0-12-385469-8.00015-0.
[2] H. Ohno, Y. Katano, Electrical properties of silicon nitride, Mater. Sci. Forum 47 (1989) 215–227, http://dx.doi.org/10.4028/www.scientific.net/MSF.47.215.
[3] J. Li, F. Chen, Q. Shen, H. Jiang, L. Zhang, Fabrication and dielectric properties of Si3N4–MgO–Al2O3 by spark plasma sintering technique, Mater. Sci.–Pol. 25 (2007) 699–707.
[4] F.L. Yu, Y. Bai, P.D. Han, Q.L. Shi, S. Ni, J.H. Wu, Spark plasma sintering of α/β Si3N4 ceramics with MgO-Al2O3 and MgO-Y2O3 as sintering additives, J. Mater. Eng. Perform. 25 (2016) 5220–5224, http://dx.doi.org/10.1007/s11665-016-2372-1.
[5] I. Khan, N. Musahwar, M. Zulfequar, Electrical and dielectric properties OF MgO-Y2O3-Si3N4 sintered ceramics, Ceramics Silik. 54 (2010) 263–268.
[6] C. Zou, C. Zhang, B. Li, S. Wang, F. Cao, Microstructure and properties of porous silicon nitride ceramics prepared by gel-casting and gas pressure sintering, Mater. Des. 44 (2013) 114–118, http://dx.doi.org/10.1016/j.matdes.2012.07.056.
[7] H. Reveron, L. Blanchard, Y. Vitupier, E. Rivière, G. Bonnefont, G. Fantozzi, Spark plasma sintering of fine alpha-silicon nitride ceramics with LAS for spatial applications, J. Eur. Ceram. Soc. 31 (2011) 645–652, http://dx.doi.org/10.1016/j.jeurceramsoc.2010.10.026.
[8] K. Berroth, Silicon nitride ceramics for product and process innovations, Adv. Sci. Technol. 65 (2010) 70–77, http://dx.doi.org/10.4028/www.scientific.net/AST.65.70.
[9] G. Ziegler, J. Heinrich, G. Wötting, Relationships between processing, microstructure and properties of dense and reaction-bonded silicon nitride, J. Mater. Sci. 22 (1987) 3041–3086.
[10] S. Hampshire, K. Jack, The kinetics of densification and phase transformation of nitrogen ceramics, Spec. Ceram. 7 (1981) 37–49.
[11] M.H. Bocanegra-Bernal, B. Matovic, Dense and near-net-shape fabrication of Si3N4 ceramics, Mater. Sci. Eng. A 500 (2009) 130–149, http://dx.doi.org/10.1016/j.msea.2008.09.015.
[12] C. Kawai, A. Yamakawa, Effect of porosity and microstructure on the strength of Si3N4: designed microstructure for high strength, high thermal shock resistance, and facile machining, J. Am. Ceram. Soc. 80 (1997) 2705–2708.
[13] H. Kawaoka, T. Adachi, T. Sekino, Y.-H. Choa, L. Gao, K. Niihara, Effect of α/β phase ratio on microstructure and mechanical properties of silicon nitride ceramics, J. Mater. Res. 16 (2001) 2264–2270.
[14] X. Zhu, H. Hayashi, Y. Zhou, K. Hirao, Influence of additive composition on thermal and mechanical properties of β–Si3N4 ceramics, J. Mater. Res. 19 (2004) 3270–3278, http://dx.doi.org/10.1557/JMR.2004.0416.
[15] B.-T. Lee, J.-H. Yoo, H.-D. Kim, Microstructural characterization of GPSed-RBSN and GPSed-Si3N4 ceramics, Mater. Trans. JIM 41 (2000) 312–316.
[16] J. Li, F. Chen, J. Niu, Y. Yang, Z. Wang, Dielectric properties of silicon nitride ceramics prepared by low temperature spark plasma sintering technique, J. Ceram. Process. Res. 12 (2011) 236–239.
[17] F.Q. Yan, F. Chen, Q. Shen, L.M. Zhang, Spark plasma sintering of α-Si3N4 ceramics with MgO-Al2O3 as sintering additives, Key Eng. Mater. 351 (2007) 176–179, http://dx.doi.org/10.4028/www.scientific.net/KEM.351.176.
[18] H. Hayashi, K. Hirao, M. Toriyama, S. Kanzaki, K. Itatani, MgSiN2 addition as a means of increasing the thermal conductivity of β-silicon nitride, J. Am. Ceram. Soc. 84 (2001) 3060–3062.
[19] T. Nishimura, M. Mitomo, H. Hirotsuru, M. Kawahara, Fabrication of silicon nitride nano-ceramics by spark plasma sintering, J. Mater. Sci. Lett. 14 (1995) 1046–1047.
[20] M.K. Park, H.N. Kim, K.S. Lee, S.S. Baek, E.S. Kang, Y.K. Baek, D.K. Kim, Effect of microstructure on dielectric properties of Si_3N_4 at microwave frequency, Key Eng. Mater. 287 (2005) 247–252, http://dx.doi.org/10.4028/www.scientific.net/KEM.287.247.
[21] O. Lukianova, Mechanical and elastic properties of new silicon nitride ceramics produced by cold isostatic pressing and free sintering, Ceram. Int. 41 (2015) 13716–13720, http://dx.doi.org/10.1016/j.ceramint.2015.08.026.
[22] V.V. Krasil'nikov, V.V. Sirota, A.S. Ivanov, L.N. Kozlova, O.A. Luk'yanova, V.V. Ivanisenko, Investigation of the structure of Si3N4-based ceramic with Al2O3 and Y2O3 additives, Glass Ceram. 71 (2014) 15–17.
[23] V. Sirota, V. Krasilnikov, O. Lukianova, Fabrication of the ceramics based on silicon nitride by free sintering and cold isostatic pressing, NANOCON 2013—Conf. Proc. (2013) 248–251.
[24] O.A. Lukianova, V.V. Krasilnikov, A.A. Parkhomenko, V.V. Sirota, Microstructure and phase composition of cold isostatically pressed and pressureless sintered silicon nitride, Nanoscale Res. Lett. 11 (2016), http://dx.doi.org/10.1186/s11671-016-1365-1.
[25] V. Sirota, O. Lukianova, V. Krasilnikov, V. Selemenev, V. Dokalov, Microstructural and physical properties of magnesium oxide-doped silicon nitride ceramics, Results Phys. 6 (2016) 82–83, http://dx.doi.org/10.1016/j.rinp.2016.01.005.
[26] O.A. Lukianova, V.V. Sirota, V.V. Krasil'nikov, A.A. Parkhomenko, Mechanical properties and microstructure of silicon nitride fabricated by pressureless sintering, in: Proceedings of IEEE International Conference on Nanomaterials Application and Properties NAP, 2016. p. 02NSA09–1. 〈http://ieeexplore.ieee.org/abstract/document/7757310/〉 (Accessed 17 September 2017).
[27] O.A. Lukianova, V.Y. Novikov, A.A. Parkhomenko, V.V. Sirota, V.V. Krasilnikov, Microstructure of spark plasma-sintered silicon nitride ceramics, Nanoscale Res. Lett. 12 (2017), http://dx.doi.org/10.1186/s11671-017-2067-z.
[28] O.A. Lukianova, V.V. Sirota, Dielectric properties of silicon nitride ceramics produced by free sintering, Ceram. Int. 43 (2017) 8284–8288, http://dx.doi.org/10.1016/j.ceramint.2017.03.161.
[29] D.R. Clarke, G. Thomas, Grain boundary phases in a hot-pressed MgO fluxed silicon nitride, J. Am. Ceram. Soc. 60 (1977) 491–495.
[30] W. Kingery, Densification during sintering in the presence of a liquid phase. I. Theory, J. Appl. Phys. 30 (1959) 301–306.
[31] C. Gazzara, Determination of phase content of silicon nitride by X-ray diffraction analysis, J. Am. Ceram. Soc. 78 (1977) 1076–1078.
[32] G. Peng, M. Liang, Z. Liang, Q. Li, W. Li, Q. Liu, Spark plasma sintered silicon nitride ceramics with high thermal conductivity using $MgSiN_2$ as additives, J. Am. Ceram. Soc. 92 (2009) 2122–2124, http://dx.doi.org/10.1111/j.1551-2916.2009.03139.x.
[33] P. Miranzo, J. González-Julián, M.I. Osendi, M. Belmonte, Enhanced particle rearrangement during liquid phase spark plasma sintering of silicon nitride-based ceramics, Ceram. Int. 37 (2011) 159–166, http://dx.doi.org/10.1016/j.ceramint.2010.08.019.
[34] B. Joshi, Z. Fu, K. Niihara, S.W. Lee, Optical, mechanical and tribological properties of Y_2O_3, Er_2O_3 and Nd_2O_3 doped polycrystalline silicon nitride ceramics, IOP Conf. Ser. Mater. Sci. Eng. 18 (2011) 082020, http://dx.doi.org/10.1088/1757-899X/18/8/082020.
[35] E. Hall, Variation of hardness of metals with grain size, Nature 173 (1954) 948–949.
[36] M.C. Chu, S. Sato, Y. Kobayashi, K. Ando, Morphological studies relating to the fracture stress and fracture toughness of silicon nitride, Fatigue Fract. Eng. Mater. Struct. 20 (1997) 829–838.
[37] A. Bellosi, J. Vicens, V. Medri, S. Guicciardi, Nanosize silicon nitride: characteristic of doped powders and of the related sintered materials, Appl. Phys. A 81 (2005) 1045–1052, http://dx.doi.org/10.1007/s00339-004-2935-0.